Engineering Analysis with Boundary Elements 29 (2005) 577–585

ENGINEERING ANALYSIS with BOUNDARY ELEMENTS

www.elsevier.com/locate/enganabound

2D Green's functions of defective magnetoelectroelastic solids under thermal loading

Qing-Hua Qin

Department of Engineering, Australian National University, Canberra, ACT 0200, Australia

Received 23 August 2004; revised 10 November 2004; accepted 24 November 2004
Available online 2 April 2005

Abstract

Thermomagnetoelectroelastic problems for various defects embedded in an infinite matrix are considered in this paper. Using Stroh's formalism, conformal mapping, and perturbation technique, Green's functions are obtained in closed form for a defect in an infinite magnetoelectroelastic solid induced by the thermal analog of a line temperature discontinuity and a line heat source. The defect may be of an elliptic hole or a Griffith crack, a half-plane boundary, a bimaterial interface, or a rigid inclusion. These Green's functions satisfy the relevant boundary or interface conditions. The proposed Green's functions can be used to establish boundary element formulation and to analyzing fracture behaviour due to the defects mentioned above.

Keywords: Green's function; Anisotropic; Half-plane; Piezoelectric/piezomagnetic; Bimaterial; Thermal stress

1. Introduction

Green's function plays an important role in the solution of numerous problems in the mechanics and physics of solids. It is the heart of many analytical and numerical methods such as singular integral equation methods, boundary element methods, eigenstrain approach, and dislocation methods [1–3]. As such, extensive studies have been carried out on static Green's functions in anisotropic piezoelectric solids. Benveniste [4] studied 3D solutions in piezoelectric solids using the Fourier transform. Chen [5] and Chen and Lin [6] expressed the infinite body Green's functions and their derivatives as the contour integrals over the unit circle using 3D Fourier transforms. Dunn [7] obtained explicit Green's functions for transversely isotropic piezoelectric solids using the Radom transform, coordinator transformation, and evaluation of residues in sequence. Pan [8] gave expressions for 2D piezoelectric Green's functions and their boundary integral equations for dealing with fracture problems. Sosa and Castro [9] obtained the solutions to the problem of concentrated loads acting at the boundary of a 2D half-plane by means of a state space method in conjunction with the Fourier transform. Norris [10] discussed the derivation of dynamic Green's functions for problems dealing with 2D dynamic piezoelectricity. Khutoryansky and Sosa [11] further examined the dynamic Green's function of piezoelectric materials and gave a general representation formula of the governing equations of transient piezoelectricity through a generalization of the reciprocal theorem and the plane wave transform method. Fan et al. [12] gave a solution for a concentrated contact force and charge acting on the boundary of a half-space by means of Stroh's formalism. The contact may be either non-slip or slip in nature. Qin [13] presented Green's functions for 2D piezoelectric materials with various openings and applied them to establish boundary singular integral equations. Qin and Mai [14] also derived explicit Green's functions for an interface crack subject to an edge dislocation in various piezoelectric bimaterial combinations. Pan and Yuan [15] gave 3D Green's functions for anisotropic piezoelectric bimaterials. They showed that the 3D bimaterial Green's function can be expressed in terms of a full-space part or the Kelvin-type solution and a complementary part or the Mindlin-type part. Studies in [6,16] suggested a numerical algorithm to compute the derivatives of the piezoelectric Green's function. Green's functions for piezoelectric materials

E-mail address: qinghua.qin@anu.edu.au.

0955-7997/$ - see front matter © 2005 Elsevier Ltd. All rights reserved.
doi:10.1016/j.enganabound.2004.11.002

without thermal effect can also be found in [17] for the case of full space; [18,19] for half-plane; [20,21] for semi-infinite crack; [22] for two-phase piezoelectric composites; [23] for anti-plane arc-crack; [24,25] for an impermeable elliptical hole or crack; [26,27] for a permeable elliptical hole; [28] for the case of collinear permeable cracks; and [29,30] for straight permeable interface cracks between two dissimilar piezoelectric media. For thermal analysis in piezoelectric materials, based on Stroh's formalism and conformal mapping, Qin [31] obtained Green's functions in closed form for an infinite piezoelectric plate with an elliptic hole induced by temperature discontinuity. Qin and Mai [32] also investigated thermoelectroelastic Green's functions for half-plane or bimaterial problems. Qin [33–35] further examined the thermoelectroelastic Green's functions for piezoelectric materials with various openings or an elliptic inclusion.

In contrast, study of corresponding Green's functions in magnetoelectroelastic solids satisfying special boundary or continuity conditions has not yet become a popular field as shown in the literature, though the solution might be of both theoretical and practical importance. Pan [36] derived three-dimensional Green's functions in anisotropic magnetoelectroelastic full-space, half-space, bimaterials based on the extended Stroh formalism and two-dimensional Fourier transforms. Pan [37] and Pan and Heyliger [38] also presented an exact solution for simply supported magneto-electro-elastic rectangular plates. Soh et al. [39] presented the 3D explicit Green's functions for an infinite three-dimensional transversely isotropic magnetoelectroelastic solid based on the potential theory. Huang et al. [40] obtained magneto-electro-elastic Eshelby tensors in an inclusion resulting from the constraint of the surrounding matrix of piezoelectric-piezomagnetic composites. Li and Dunn [41] and Li [42] studied coupled magneto-electroelastic behaviour due to inclusion or inhomogeneity using Eshelby's tensor approach. Hou et al. [43] presented a general solution for transversely isotropic magneto-electro-elastic media in terms of five harmonic functions. Based on Stroh's formalism, comformal mapping, and Laurent series expansion, Liu et al. [44] obtained Green's functions for an infinite 2D anisotropic magneto-electro-elastic medium containing an elliptical cavity or a crack. To the author's knowledge, however, there is no report on thermal Green's function for media possessing simultaneously piezoelectric, piezomagnetic, magneto-electric, and thermal effects. In the present paper, thermal Green's functions for 2D anisotropic magneto-electro-elastic solids with various defects are presented. The defects may be an elliptic hole or a Griffith crack, a half-plane boundary, a bimaterial interface, or a rigid inclusion. The Green's functions presented here are suitable for implementing into standard boundary element formulation and computer programming for numerical analysis.

2. Basic formulations

The governing equations and general solutions of 2D magnetoelectroelastic solids where all fields are functions of x_1 and x_2 only are here summarized briefly. Throughout this paper the shorthand notation introduced by Barnett and Lothe [45] and the fixed Cartesian coordinate system (x_1, x_2, x_3) are adopted. Lower case Latin subscripts always range from 1 to 3, upper case Latin subscripts will range from 1 to 5, and the summation convention is used for repeating subscripts unless otherwise indicated. In the stationary case where no free electric charge, electric current, body force, and heat source are assumed to exist, the complete set of governing equations for coupled thermo-electro-magneto-elastic problems are [46,47]:

$$h_{i,i} = 0 \quad \Sigma_{iJ,i} = 0 \tag{1}$$

together with

$$h_i = -k_{ij}T_{,j} \quad \Sigma_{iJ} = E_{iJMn}U_{M,n} - \chi_{iJ}T \tag{2}$$

in which

$$\Sigma_{iJ} = \begin{cases} \sigma_{ij}, & J\le 3, \\ D_i, & J=4, \\ B_i, & J=5, \end{cases} \quad U_M = \begin{cases} u_m, & M\le 3, \\ \phi, & M=4, \\ \varpi, & M=5, \end{cases}$$
$$\chi_{iJ} = \begin{cases} \lambda_{ij}, & J\le 3, \\ \rho_i, & J=4, \\ \upsilon_i, & J=5, \end{cases} \tag{3}$$

$$E_{iJMn} = \begin{cases} C_{ijmn}, & J,M\le 3, \\ e_{nij}, & J\le 3, M=4, \\ q_{nij}, & J\le 3, M=5, \\ e_{imn}, & J=4, M\le 3, \\ -\kappa_{in}, & J=4, M=4, \\ -a_{in}, & J=4, M=5, \\ q_{imn}, & J=5, M\le 3, \\ -a_{in}, & J=5, M=4, \\ -\mu_{in} & J=5, M=5, \end{cases} \tag{4}$$

where T and h_i are temperature change and heat flux, σ_{ij}, D_i, and B_i are elastic stress tensor, electric displacement vector, and magnetic induction vector; u_m, ϕ, and ϖ are elastic displacement vector, electric potential, and magnetic potential; λ_{ij}, ρ_i, and υ_i are thermal moduli tensor, pyroelectric coefficients, and pyromagnetic coefficients; k_{ij} is the thermal conductivity; C_{ijmn} elastic moduli, e_{nij} piezoelectric coefficients, q_{nij} piezomagnetic coefficients, a_{in} magnetoelectric coefficients, κ_{in} dielectric constants, μ_{in} magnetic permeability. A general solution to Eq. (1) can be expressed as [47]:

$$T = 2\,\mathrm{Re}[g'(z_t)], \quad \mathbf{U} = 2\,\mathrm{Re}[\mathbf{Af}(\mathbf{z})\mathbf{q} + \mathbf{c}g(z_t)] \tag{5}$$

with

$$\mathbf{A} = [\mathbf{A}_1\ \mathbf{A}_2\ \mathbf{A}_3\ \mathbf{A}_4\ \mathbf{A}_5]$$
$$\mathbf{f}(\mathbf{z}) = \langle f(z_\alpha)\rangle = \mathrm{diag}[f(z_1)\,f(z_2)\,f(z_3)\,f(z_4)\,f(z_5)]$$
$$\mathbf{q} = \{q_1\ q_2\ q_3\ q_4\ q_5\}^T$$
$$z_t = x_1 + \tau x_2$$
$$z_i = x_1 + p_i x_2$$

in which 'Re' stands for the real part of the complex number, the prime ($'$) denotes differentiation with the argument, $\mathbf{q}$ represents unknown constants to be found by boundary conditions, g and $\mathbf{f}$ are arbitrary functions to be determined, p_i, τ, $\mathbf{A}$ and $\mathbf{c}$ are constants determined by [2]

$$\begin{aligned} &k_{22}\tau^2 + (k_{12} + k_{21})\tau + k_{11} = 0 \\ &[\mathbf{Q} + (\mathbf{R} + \mathbf{R}^T)p_i + \mathbf{T}p_i^2]\mathbf{A}_i = 0 \\ &[\mathbf{Q} + (\mathbf{R} + \mathbf{R}^T)\tau + \mathbf{T}\tau^2]\mathbf{c} = \boldsymbol{\chi}_1 + \tau\boldsymbol{\chi}_2 \end{aligned} \tag{6}$$

in which superscript 'T' denotes the transpose, $\boldsymbol{\chi}_i$ are 5×1 vectors, and $\mathbf{Q}$, $\mathbf{R}$ and $\mathbf{T}$ are 5×5 matrices defined by

$$\begin{aligned} &\boldsymbol{\chi}_i = \{\lambda_{i1}\ \lambda_{i2}\ \lambda_{i3}\ \rho_i\ \upsilon_i\}^T, \quad (\mathbf{Q})_{IK} = E_{1IK1}, \\ &(\mathbf{R})_{IK} = E_{1IK2}, \quad (\mathbf{T})_{IK} = E_{2IK2} \end{aligned} \tag{7}$$

The heat flux, $\mathbf{h}$, and the stress-electric displacement-magnetic induction (SEDMI), $\boldsymbol{\Sigma}$, obtained from Eq. (2) can be written as

$$\begin{aligned} &h_i = -2\,\mathrm{Re}[(k_{i1} + \tau k_{i2})g''(z_t)], \\ &\boldsymbol{\Sigma}_{1J} = -\boldsymbol{\phi}_{J,2}, \quad \boldsymbol{\Sigma}_{2J} = \boldsymbol{\phi}_{J,1} \end{aligned} \tag{8}$$

where $\boldsymbol{\phi}$ is the SEDMI function given as

$$\boldsymbol{\phi} = 2\,\mathrm{Re}[\mathbf{Bf}(\mathbf{z})\mathbf{q} + \mathbf{d}g(z_t)] \tag{9}$$

with

$$\begin{aligned} &\mathbf{B} = \mathbf{R}^T\mathbf{A} + \mathbf{TAP} = -(\mathbf{QA} + \mathbf{RAP})\mathbf{P}^{-1} \\ &\mathbf{P} = \langle p_\alpha\rangle = \mathrm{diag}[p_1\ p_2\ p_3\ p_4\ p_5] \\ &\mathbf{d} = (\mathbf{R}^T + \tau\mathbf{T})\mathbf{c} - \boldsymbol{\chi}_2 = -(\mathbf{Q} + \tau\mathbf{R})\mathbf{c}/\tau + \boldsymbol{\chi}_1/\tau \end{aligned} \tag{10}$$

Introducing a heat flow function [34]

$$\vartheta = 2k\,\mathrm{Im}[g'(z_t)] \tag{11}$$

where $k = (k_{11}k_{22} - k_{12}^2)^{1/2}$, 'Im' stands for the imaginary part of the complex number, we have

$$h_1 = -\vartheta_{,2}, \quad h_2 = \vartheta_{,1} \tag{12}$$

which has the same form as those for stress function (see Eq. $(8)_2$). Thus we may use the same method as that in electroelastic problems to derive the thermal solutions.

3. Green's function for half-plane or bimaterial problems

3.1. Green's function for half-plane problem

The half-plane considered here is slightly different from those reported in the literature [2,18]. The half-plane boundary is in the vertical direction ($x_1 = 0$ on the boundary in our analysis), rather than in the horizontal direction (see Fig. 1). It is obvious that $z_t = x_1 + \tau x_2$ (or $z_k = x_1 + p_k x_2$) becomes a real number on the horizontal boundary $x_2 = 0$. However, z_t (or z_k) is, in general, neither a real number nor a pure imaginary number on the vertical boundary $x_1 = 0$, which makes the related mathematical derivation complicated. To bypass this problem, introduce a new coordinate variable

$$z_t^* = z_t/\tau, \quad z_k^* = z_k/p_k \tag{13}$$

which makes both z_t^* and z_k^* to be real numbers on the vertical boundary $x_1 = 0$. This coordinate transformation is used for both the half-plane and the bimaterial problem.

In the analysis the boundary faces of the half-plane are assumed to be thermal-insulated, free of traction force, external electric current and charge. The boundary condition along the boundary of the half-plane can thus be written as

$$\vartheta = \boldsymbol{\phi} = 0 \tag{14}$$

Here following relations have been used

$$h_n = \vartheta_{,s}, \quad \mathbf{t}_n = \boldsymbol{\phi}_{,s} \tag{15}$$

where n is the normal direction of the half-plane boundary, s is the arc length measured along the boundary face, and $\mathbf{t}_n$ represents surface traction vector.

3.1.1. Green's function for thermal field in half-plane solid

The half-plane solution can be obtained by considering full-space solution plus some modification term to satisfy

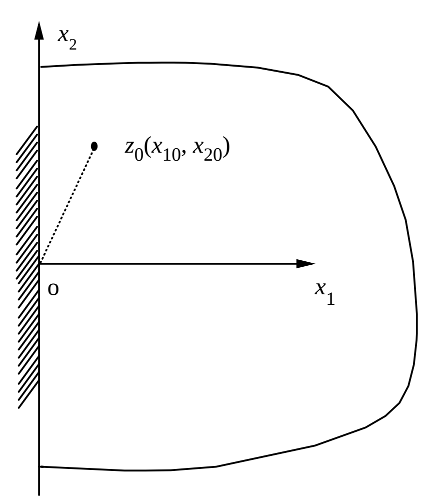

Fig. 1. Magnetoelectroelastic half-plane.

the condition on the boundary of the half-plane. To this end, the general solution for temperature and heat-flow function can be assumed in the form [34]

$$T = 2\,\mathrm{Re}[g'(z_t^*)] = 2\,\mathrm{Re}[f_0(z_t^*) + f_1(z_t^*)] \tag{16}$$

$$\vartheta = 2k\,\mathrm{Im}[g'(z_t^*)] = 2k\,\mathrm{Im}[f_0(z_t^*) + f_1(z_t^*)] \tag{17}$$

where f_0 can be chosen to represent the solutions associated with the unperturbed thermal fields which are holomorphic in the entire domain except at some singular points such as the point at which a point heat source is applied, and f_1 is a function corresponding to the perturbed field due to the half-plane.

For a given loading condition, the full plane function f_0 can be obtained easily since it is related to the solution of homogeneous media. When an infinite plane is subjected to a line heat source h^* and the thermal analog of a line temperature discontinuity T_0 both located at (x_{10}, x_{20}), the function f_0 can be chosen in the form

$$f_0(z_t^*) = q_0 \ln(z_t^* - z_{t0}^*) \tag{18}$$

and q_0 is a complex number which can be determined from the conditions

$$\int_C \mathrm{d}T = T_0 \text{ for any closed curve } C \text{ enclosing the point } z_{t0}^*, \tag{19}$$

$$\int_C \mathrm{d}\vartheta = -h^* \text{ for any closed curve } C \text{ enclosing the point } z_{t0}^*. \tag{20}$$

with the substitution of Eq. (18) into Eqs. (16) and (17), the conditions (19) and (20) yield

$$q_0 = T_0/4\pi i - h^*/4\pi k. \tag{21}$$

For the half-plane in the $z_t^* = z_t/\tau$ system, the perturbation function can be assumed in the form [2,32]

$$f_1(z_t^*) = q_1 \ln(z_t^* - \bar{z}_{t0}^*) \tag{22}$$

Substituting Eqs. (18) and (22) into Eq. (17), the condition $(14)_1$ yields

$$\mathrm{Im}[q_0 \ln(x_2 - z_{t0}^*) + q_1 \ln(x_2 - \bar{z}_{t0}^*)] = 0 \tag{23}$$

Noting that $z_t^* = x_2$ on the half-plane boundary and $\mathrm{Im}(f) = -\mathrm{Im}(\bar{f})$, we have

$$\mathrm{Im}[q_0 \ln(x_2 - z_{t0}^*)] = -\mathrm{Im}[\bar{q}_0 \ln(x_2 - \bar{z}_{t0}^*)] \tag{24}$$

Eq. (23) now yields

$$q_1 = \bar{q}_0 \tag{25}$$

The function g in Eq. (16) can then be obtained by integrating f_0 and f_1 with respect to z_t, which yields

$$g(z_t) = q_0\hat{f}(z_t^*, z_{t0}^*) + \bar{q}_0\hat{f}(z_t^*, \bar{z}_{t0}^*) \tag{26}$$

where $\hat{f}(x,a) = (x-a)[\ln(x-a) - 1]$.

3.1.2. Green's function for magnetoelectroelastic field in half-plane solid

The general solution of the thermomagnetoelectroelastic problem can be written as

$$\mathbf{U} = \mathbf{U}_\mathrm{p} + \mathbf{U}_\mathrm{h}, \quad \boldsymbol{\phi} = \boldsymbol{\phi}_\mathrm{p} + \boldsymbol{\phi}_\mathrm{h} \tag{27}$$

where subscripts 'p' and 'h' refer, respectively, to the particular and homogeneous solution.

From Eqs. (5) and (9) the particular solution of magnetoelectroelastic field induced by thermal loading can be written as

$$\mathbf{u}_p = 2\,\mathrm{Re}[\mathbf{c}g(z_t)], \quad \boldsymbol{\phi}_p = 2\,\mathrm{Re}[\mathbf{d}g(z_t)] \tag{28}$$

The particular solutions (28) do not generally satisfy the boundary condition $(14)_2$ along the half-plane boundary. We therefore need to seek a corrective isothermal solution for a given problem so that, when superimposed on the particular thermomagnetoelectroelastic solution, the surface conditions $(14)_2$ will be satisfied. Owing to the fact that $f(z_k)$ and $g(z_t)$ have the same order of effect on stress and electric displacement in Eqs. (5) and (9), possible function forms come from the partition of $g(z_t)$. The corrective isothermal solution $\mathbf{U}_\mathrm{h}$ and $\boldsymbol{\phi}_\mathrm{h}$ can, thus, be assumed in the form

$$\mathbf{U}_\mathrm{h} = 2\,\mathrm{Re}[\mathbf{c}q_0\hat{f}(z_k^*, z_{t0}^*) + \mathbf{c}\bar{q}_0[\hat{f}(z_k^*, \bar{z}_{t0}^*)] \tag{29}$$

$$\boldsymbol{\phi}_\mathrm{h} = 2\,\mathrm{Re}[\mathbf{d}q_0\hat{f}(z_k^*, z_{t0}^*)] + \mathbf{d}\bar{q}_0\hat{f}(z_k^*, \bar{z}_{t0}^*)] \tag{30}$$

For Simplicity, denote

$$f(z_k^*) = q_0[\hat{f}(z_k^*, z_{t0}^*) + \bar{q}_0\hat{f}(z_k^*, \bar{z}_{t0}^*)] \tag{31}$$

The substitution of Eqs. (29)–(31) into (9), later into $(14)_2$, leads to

$$\mathbf{q} = -\mathbf{B}^{-1}\mathbf{d} \tag{32}$$

Thus Green's functions for the magnetoelectroelastic field of the half-plane problem can be written as

$$\begin{aligned} \mathbf{U} &= 2\,\mathrm{Re}[-\mathbf{A}\mathbf{f}(\mathbf{z}^*)\mathbf{B}^{-1}\mathbf{d} + \mathbf{c}g(z_t)], \\ \boldsymbol{\phi} &= 2\,\mathrm{Re}[-\mathbf{B}\mathbf{f}(\mathbf{z}^*)\mathbf{B}^{-1}\mathbf{d} + \mathbf{d}g(z_t)] \end{aligned} \tag{33}$$

where $\mathbf{f}(\mathbf{z}^*) = \mathrm{diag}[f(z_1^*)\, f(z_2^*)\, f(z_3^*)\, f(z_4^*)\, f(z_5^*)]$.

3.2. Green's function for bimaterial problem

We now consider a bimaterial solid whose interface is on x_2-axis ($x_1 = 0$). It is assumed that the left half-plane ($x_1 < 0$) is occupied by material 1, and the right half plane ($x_1 > 0$) is occupied by material 2 (Fig. 2). They are rigidly bonded together so that

$$\begin{aligned} &T^{(1)} = T^{(2)}, \quad \vartheta^{(1)} = \vartheta^{(2)}, \quad \mathbf{U}^{(1)} = \mathbf{U}^{(2)}, \\ &\boldsymbol{\phi}^{(1)} = \boldsymbol{\phi}^{(2)}, \text{ at } x_1 = 0 \end{aligned} \tag{34}$$

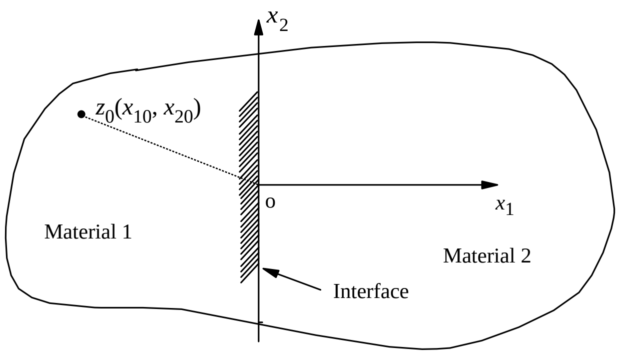

Fig. 2. Magnetoelectroelastic bimaterial plate.

where the superscripts (1) and (2) label the quantities relating to materials 1 and 2 respectively. The equality of heat flow and traction continuity comes from the relations $h_n = \partial\vartheta/\partial s$ and $\mathbf{t} = \partial\boldsymbol{\phi}/\partial s$. When points along the interface are considered, integration of $h_n^{(1)} = h_n^{(2)}$ and $\mathbf{t}^{(1)} = \mathbf{t}^{(2)}$ provides Eq. $(34)_{2,4}$, since the integration constants which correspond to constant thermal expansion and rigid motion can be neglected.

3.2.1. Green's function for thermal field in bimaterial solids

For a bimaterial subjected to a temperature discontinuity T_0 and a heat source h^*, both located in the left half-plane at z_0 (x_{10}, x_{20}) as shown in Fig. 2, the general solution for the bimaterial solid can be assumed in the form

$$\begin{aligned} T^{(1)} &= 2\,\mathrm{Re}[f_0(z_t^{(1)*}) + f_1(z_t^{(1)*})], \\ \vartheta^{(1)} &= 2k^{(1)}\,\mathrm{Im}[f_0(z_t^{(1)*}) + f_1(z_t^{(1)*})], \quad x_1 < 0, \end{aligned} \tag{35}$$

$$T^{(2)} = 2\,\mathrm{Re}[f_2(z_t^{(2)*})], \quad \vartheta^{(2)} = 2k^{(2)}\,\mathrm{Im}[f_2(z_t^{(2)*})], \quad x_1 > 0 \tag{36}$$

where the function f_0 is again given in Eq. (18). To satisfy the interface condition $(34)_{1,2}$, the functions f_1 and f_2 are taken as

$$f_1(z_t^{(1)*}) = q_1 \ln(z_t^{(1)*} - \bar{z}_{t0}^{(1)*}) \tag{37}$$

$$f_2(z_t^{(2)*}) = q_2 \ln(z_t^{(2)*} - z_{t0}^{(1)*}) \tag{38}$$

with the substitution of Eqs. (18), (37), and (38) into Eqs. (35) and (36), the continuity condition $(34)_{1,2}$ provides

$$q_1 = \frac{k^{(1)} - k^{(2)}}{k^{(2)} + k^{(1)}}\bar{q}_0, \quad q_2 = \frac{2k^{(1)}}{k^{(1)} + k^{(2)}} q_0 \tag{39}$$

Therefore the function g for the present bimaterial problem can be written in the form

$$g_1(z_t^{(1)*}) = q_0 \hat{f}(z_t^{(1)*}, z_{t0}^{(1)*}) + q_1 \hat{f}(z_t^{(1)*}, \bar{z}_{t0}^{(1)*}) \tag{40}$$

$$g_2(z_t^{(2)*}) = q_2 \hat{f}(z_t^{(2)*}, z_{t0}^{(1)*}) \tag{41}$$

3.2.2. Green's function for magnetoelectroelastic field in bimaterial solids

To use the condition $(34)_{3,4}$ we first consider the particular solution due to the thermal field. Using Eqs. (40) and (41), the particular solution for the magnetoelectroelastic field can be written as

$$\mathbf{U}_p^{(1)}(z_t^{(1)*}) = 2\,\mathrm{Re}[q_0 \mathbf{c}^{(1)} \hat{f}(z_t^{(1)*}, z_{t0}^{(1)*}) + \mathbf{c}^{(1)} q_1 [\hat{f}(z_t^{(1)*}, \bar{z}_{t0}^{(1)*})], \tag{42}$$

$$\boldsymbol{\phi}_p^{(1)}(z_t^{(1)*}) = 2\,\mathrm{Re}[q_0 \mathbf{d}^{(1)} \hat{f}(z_t^{(1)*}, z_{t0}^{(1)*}) + \mathbf{d}^{(1)} q_1 \hat{f}(z_t^{(1)*}, \bar{z}_{t0}^{(1)*})] \tag{43}$$

for $x_1 < 0$, and

$$\mathbf{U}_p^{(2)}(z_t^{(2)*}) = 2\,\mathrm{Re}[\mathbf{c}^{(2)} q_2 \hat{f}(z_t^{(2)*}, z_{t0}^{(1)*})], \tag{44}$$

$$\boldsymbol{\phi}_p^{(2)}(z_t^{(2)*}) = 2\,\mathrm{Re}[\mathbf{d}^{(2)} q_2 \hat{f}(z_t^{(2)*}, z_{t0}^{(1)*})] \tag{45}$$

for $x_1 > 0$. For the same reason as in Section 3.1.2, a corrective solution needs to be constructed in such a way that when it is superimposed on the particular solutions (42)–(45) the interface condition (34) will be satisfied. Owing to the fact that $f(z_k)$ and $g(z_t)$ have the same rule affecting $\mathbf{U}$ and $\boldsymbol{\phi}$ in Eqs. (5) and (9), possible function forms come from the partition of solution $g(z_t)$. This is

$$f_1(z_k^{(1)*}) = \hat{f}(z_k^{(1)*}, z_{t0}^{(1)*}), \quad f_2(z_k^{(1)*}) = \hat{f}(z_k^{(1)*}, \bar{z}_{t0}^{(1)*}) \tag{46}$$

$$f_3(z_k^{(2)*}) = \hat{f}(z_k^{(2)*}, z_{t0}^{(1)*}), \quad f_4(z_k^{(2)*}) = \hat{f}(z_k^{(2)*}, \bar{z}_{t0}^{(1)*}) \tag{47}$$

Thus the resulting expressions of $\mathbf{U}^{(i)}$ and $\boldsymbol{\phi}^{(i)}$ can be given as

$$\begin{aligned} \mathbf{U}^{(1)} = 2\,\mathrm{Re}\{&\mathbf{A}^{(1)}[\langle f_1(z_\alpha^{(1)*})\rangle \mathbf{q}_{11} + \langle f_2(z_\alpha^{(1)*})\rangle \mathbf{q}_{12}] \\ &+ q_0 \mathbf{c}^{(1)} \hat{f}(z_t^{(1)*}, z_{t0}^{(1)*}) + \mathbf{c}^{(1)} q_1 \hat{f}(z_t^{(1)*}, \bar{z}_{t0}^{(1)*})\} \end{aligned} \tag{48}$$

$$\begin{aligned} \boldsymbol{\phi}^{(1)} = 2\,\mathrm{Re}\{&\mathbf{B}^{(1)}[\langle f_1(z_\alpha^{(1)*})\rangle \mathbf{q}_{11} + \langle f_2(z_\alpha^{(1)*})\rangle \mathbf{q}_{12}] \\ &+ q_0 \mathbf{d}^{(1)} \hat{f}(z_t^{(1)*}, z_{t0}^{(1)*}) + \mathbf{d}^{(1)} q_1 \hat{f}(z_t^{(1)*}, \bar{z}_{t0}^{(1)*})\} \end{aligned} \tag{49}$$

for $x_1 < 0$, and

$$\begin{aligned} \mathbf{U}^{(2)} = 2\,\mathrm{Re}\{&\mathbf{A}^{(2)}[\langle f_3(z_\alpha^{(2)*})\rangle \mathbf{q}_{21} + \langle f_4(z_\alpha^{(2)*})\rangle \mathbf{q}_{22}] \\ &+ \mathbf{c}^{(2)} q_2 \hat{f}(z_t^{(2)*}, z_{t0}^{(1)*})\} \end{aligned} \tag{50}$$

$$\begin{aligned} \boldsymbol{\phi}^{(2)} = 2\,\mathrm{Re}\{&\mathbf{B}^{(2)}\langle f_3(z_\alpha^{(2)*})\rangle \mathbf{q}_{21} + \langle f_4(z_\alpha^{(2)*})\rangle \mathbf{q}_{22}] \\ &+ \mathbf{d}^{(2)} q_2 \hat{f}(z_t^{(2)*}, z_{t0}^{(1)*})\} \end{aligned} \tag{51}$$

for $x_1 > 0$. The substitution of Eqs. (48)–(51) into Eq. $(34)_{3,4}$ yields

$$\begin{aligned} \mathbf{q}_{11} = \mathbf{M}_1[&(\mathbf{B}^{(2)-1}\mathbf{d}^{(2)} - \mathbf{A}^{(2)-1}\mathbf{c}^{(2)}) q_2 - (\mathbf{B}^{(2)-1}\mathbf{d}^{(1)} \\ &- \mathbf{A}^{(2)-1}\mathbf{c}^{(1)}) q_0] \end{aligned} \tag{52}$$

$$\mathbf{q}_{21} = \mathbf{M}_2[(\mathbf{B}^{(1)-1}\mathbf{d}^{(1)} - \mathbf{A}^{(1)-1}\mathbf{c}^{(1)})q_0 - (\mathbf{B}^{(1)-1}\mathbf{d}^{(2)} - \mathbf{A}^{(1)-1}\mathbf{c}^{(2)})q_2] \tag{53}$$

$$\mathbf{q}_{12} = -\mathbf{M}_1(\mathbf{B}^{(2)-1}\mathbf{d}^{(1)} - \mathbf{A}^{(2)-1}\mathbf{c}^{(1)})q_1 \tag{54}$$

$$\mathbf{q}_{22} = \mathbf{M}_2(\mathbf{B}^{(1)-1}\mathbf{d}^{(1)} - \mathbf{A}^{(1)-1}\mathbf{c}^{(1)})q_1 \tag{55}$$

where $\mathbf{M}_1 = (\mathbf{B}^{(2)-1}\mathbf{B}^{(1)} - \mathbf{A}^{(2)-1}\mathbf{A}^{(1)})^{-1}$, $\mathbf{M}_2 = (\mathbf{B}^{(1)-1}\mathbf{B}^{(2)} - \mathbf{A}^{(1)-1}\mathbf{A}^{(2)})^{-1}$. Thus, the explicit expression of the magnetothermoelectroelastic Green's functions for the bimaterial solid can be obtained by substituting Eqs. (52)–(55) into Eqs. (48)–(51).

4. Green's function for elliptical hole or rigid inclusion problem

4.1. Green's function for elliptical hole problem

The hole problem to be considered here is illustrated in Fig. 3, showing an infinite two-dimensional thermomagnetoelectroelastic plate containing an elliptical hole (with the limit $b=0$, a crack) with semi-major axis a and semi-minor axis b. The plate is subjected to a line heat source h^* and the thermal analog of a line temperature discontinuity T_0, both located at $z_0(x_{10}, x_{20})$ (Fig. 3).

As shown in Fig. 3, the contour Γ of the ellipse is described by

$$x_1 = a\cos\psi, \quad x_2 = b\sin\psi \tag{56}$$

where ψ is a real parameter. Letting $\mathbf{m}$ and $\mathbf{n}$ be the unit vectors tangential and normal to the elliptical boundary, respectively, and ω be the angle directed counter-clockwise from the positive x_1-axis to the unit vector $\mathbf{m}$, we have

$$\mathbf{m} = \{\cos\omega, \sin\omega, 0\}^T, \quad \mathbf{n} = \{-\sin\omega, \cos\omega, 0\}^T \tag{57}$$

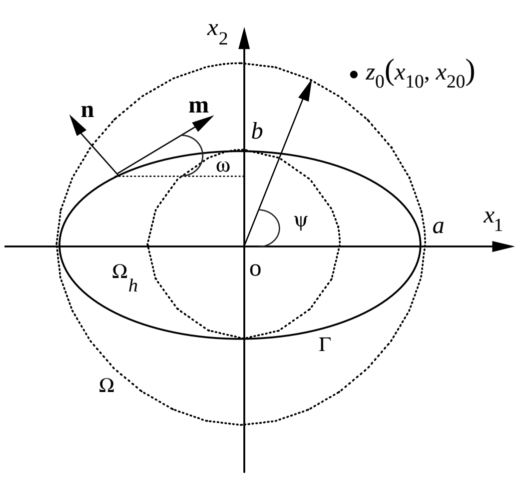

Fig. 3. Geometry of an ellipse.

The normal component of SEDMI vector along the hole boundary can then be expressed as

$$(\boldsymbol{\Sigma}_n)_J = \Sigma_{iJ}n_i = (\boldsymbol{\phi}_{,m})_J \tag{58}$$

If it is assumed that the hole surface is thermal insulated and SEDMI free, the physical and boundary conditions of the boundary-value problem can be stated as

$$\int_C \mathrm{d}T = T_0 \text{ for any closed curve } C \text{ enclosing the point } z_0 \tag{59}$$

$$\int_C \mathrm{d}\vartheta = -h^* \text{ for any closed curve } C \text{ enclosing the point } z_0 \tag{60}$$

$$\vartheta = \boldsymbol{\phi} = 0 \text{ along the hole boundary} \tag{61}$$

$$h_i \to 0, \quad \Sigma_{iJ} \to 0 \text{ at infinity} \tag{62}$$

4.1.1. Conformal mapping

Since conformal mapping is a fundamental tool used to find the solution of hole problems, the transformation

$$z_t = a_{1\tau}\zeta_t + a_{2\tau}\zeta_t^{-1}, \quad a_{1\tau} = (a - \mathrm{i}\tau b)/2, \quad a_{2\tau} = (a + \mathrm{i}\tau b)/2 \tag{63}$$

$$z_k = a_{1k}\zeta_k + a_{2k}\zeta_k^{-1}, \quad a_{1k} = (a - \mathrm{i}p_k b)/2, \quad a_{2k} = (a + \mathrm{i}p_k b)/2 \tag{64}$$

will be used to map the region, Ω, occupied by the magnetoelectroelastic material onto the outside of a unit circle in the ζ-plane, described by $\zeta_\alpha|_\Gamma = \sigma$. It is noted that ζ_α on the unit circle is expressed by

$$\zeta_\alpha|_\Gamma = \mathrm{e}^{\mathrm{i}\psi} = \cos\psi + \mathrm{i}\sin\psi\,(\alpha = t, 1-5) \tag{65}$$

4.1.2. Green's function for thermal field in hole problem

A suitable function satisfying the boundary conditions (59), (60), and $(62)_1$, can be given in the form

$$g'(\zeta_t) = q_0 \ln(\zeta_t - \zeta_{t0}) + q_1 \ln(\zeta_t^{-1} - \bar{\zeta}_{t0}) \tag{66}$$

where q_0 is defined in Eq. (21). Noting that $\bar{\zeta}_t = \bar{\sigma} = \sigma^{-1}$, we have

$$\mathrm{Im}[q_0 \ln(\sigma - \zeta_{t0})] = -\mathrm{Im}[\bar{q}_0 \ln(\sigma^{-1} - \bar{\zeta}_{t0})] \tag{67}$$

The substitution of Eq. (67) into Eq. (66), and then into Eq. $(61)_1$, yields

$$q_1 = \bar{q}_0 \tag{68}$$

The function $g(z_t)$ is thus obtained by integrating Eq. (66) with respect to z_t, i.e.

$$g(z_t) = \int g'(z_t)\mathrm{d}\,z_t = \int g'(\zeta_t)(a_{1\tau} - a_{2\tau}\zeta_t^{-2})\mathrm{d}\,\zeta_t \tag{69}$$

which yields

$$g(z_t)=q_0\{a_{1\tau}(\zeta_t-\zeta_{t0})[\ln(\zeta_t-\zeta_{t0})-1]-a_{2\tau}[\ln(\zeta_t-\zeta_{t0})-\ln\zeta_t]/\zeta_{t0}+a_{2\tau}\zeta_t^{-1}\ln(\zeta_t-\zeta_{t0})\}+q_1\{a_{1\tau}\zeta_t\ln(\zeta_t^{-1}-\bar{\zeta}_{t0})-a_{1\tau}[\ln(\zeta_t^{-1}-\bar{\zeta}_{t0})+\ln\zeta_t]/\bar{\zeta}_{t0}+a_{2\tau}(\zeta_t^{-1}-\bar{\zeta}_{t0})[\ln(\zeta_t^{-1}-\bar{\zeta}_{t0})-1]\} \tag{70}$$

4.1.3. Green's function for magnetoelectroelastic field in hole problem

As before, the particular solution is in the same form as that of Eq. (28) except for the function g being obtained from Eq. (70). Based on the Eq. (70), the corrective isothermal solution can be taken in the form

$$\begin{aligned} f_1(z_k) &= a[q_0F_1(\zeta_k)+q_0F_2(\zeta_k)+\bar{q}_0F_3(\zeta_k)+\bar{q}_0F_4(\zeta_k)]/2 \\ f_2(z_k) &= ip_kb[-q_0F_1(\zeta_k)+q_0F_2(\zeta_k)-\bar{q}_0F_3(\zeta_k)+\bar{q}_0F_4(\zeta_k)]/2 \end{aligned} \tag{71}$$

where the subscripts 1 and 2 are the indices for the different possible functions, and

$$\begin{aligned} F_1(\zeta_k) &= (\zeta_k-\zeta_{t0})[\ln(\zeta_k-\zeta_{t0})-1], \\ F_2(\zeta_k) &= (\zeta_k^{-1}-\zeta_{t0}^{-1})\ln(\zeta_k-\zeta_{t0})+\zeta_{t0}^{-1}\ln\zeta_k, \\ F_3(\zeta_k) &= (\zeta_k^{-1}-\bar{\zeta}_{t0})[\ln(\zeta_k^{-1}-\bar{\zeta}_{t0})-1], \\ F_4(\zeta_k) &= (\zeta_k-\bar{\zeta}_{t0}^{-1})\ln(\zeta_k^{-1}-\bar{\zeta}_t^*)-\bar{\zeta}_{t0}^{-1}\ln\zeta_k \end{aligned} \tag{72}$$

The Green's functions for the magnetoelectroelastic fields can thus be chosen as

$$\mathbf{U}=2\,\mathrm{Re}\left[\sum_{k=1}^{2}\mathbf{A}\mathbf{f}_k(\mathbf{z})\mathbf{q}_k+\mathbf{c}g(z_t)\right] \tag{73}$$

$$\boldsymbol{\phi}=2\,\mathrm{Re}\left[\sum_{k=1}^{2}\mathbf{B}\mathbf{f}_k(\mathbf{z})\mathbf{q}_k+\mathbf{d}g(z_t)\right] \tag{74}$$

The condition $(61)_2$ provides

$$\mathbf{q}_1=-\mathbf{B}^{-1}\mathbf{d},\quad \mathbf{q}_2=-\tau\mathbf{P}^{-1}\mathbf{B}^{-1}\mathbf{d} \tag{75}$$

Substituting Eq. (75) into Eqs. (73) and (74), the Green's functions can then be rewritten as

$$\mathbf{U}=2\,\mathrm{Re}\{-\mathbf{A}[\mathbf{f}_1(\mathbf{z})+\mathbf{f}_2(\mathbf{z})\mathbf{P}^{-1}\tau]\mathbf{B}^{-1}\mathbf{d}+\mathbf{c}g(z_t)\} \tag{76}$$

$$\boldsymbol{\phi}=2\,\mathrm{Re}\{-\mathbf{B}[\mathbf{f}_1(\mathbf{z})+\mathbf{f}_2(\mathbf{z})\mathbf{P}^{-1}\tau]\mathbf{B}^{-1}\mathbf{d}+\mathbf{d}g(z_t)\} \tag{77}$$

In the case of the elliptical hole being filled with a rigid conductor, which implies that the elliptical hole is not deformed and the electrical potential as well as the magnetic potential is constant (=0 in this study) on the hole surface, we have

$$\mathbf{U}|_\Gamma=0 \tag{78}$$

The unknown constants in Eq. (73) are then given by

$$\mathbf{q}_1=-\mathbf{A}^{-1}\mathbf{c},\quad \mathbf{q}_2=-\tau\mathbf{P}^{-1}\mathbf{A}^{-1}\mathbf{c} \tag{79}$$

when the minor semi-axis b of the ellipse approaches zero, the hole reduces to a flat crack of length $2a$. The Green's functions (76) and (77) in this case are reduced to

$$\mathbf{U}=2\,\mathrm{Re}\{-\mathbf{A}\mathbf{f}_1(\mathbf{z})\mathbf{B}^{-1}\mathbf{d}+\mathbf{c}g(z_t)\} \tag{80}$$

$$\boldsymbol{\phi}=2\,\mathrm{Re}\{-\mathbf{B}\mathbf{f}_1(\mathbf{z})\mathbf{B}^{-1}\mathbf{d}+\mathbf{d}g(z_t)\} \tag{81}$$

4.1.4. Green's function for permeable hole problem

In this subsection, the hole is assumed to be filled with a homogeneous gas (air or vacuum) of permittivity (κ^h) and permeability (μ^h), where superscript 'h' refers to the quantities associated with the hole [27,44]. Therefore, induced electric and magnetic fields exist in the hole, denoted by Ω_h, and can be governed by the equations:

$$\nabla^2\phi^h=0,\quad \nabla^2\psi^h=0 \text{ in } \Omega_h \tag{82}$$

with the constitutive relations

$$D_i^h=\kappa^hE_i^h=-\kappa^h\phi_{,i}^h,\quad B_i^h=\kappa^hH_i^h=-\mu^h\psi_{,i}^h\quad i=1,2 \text{ in } \Omega_h \tag{83}$$

The general solution to Eqs. (82) and (83) are thus given by

$$\phi^h=2\,\mathrm{Re}[f_1^h(z)],\quad \psi^h=2\,\mathrm{Re}[f_2^h(z)],\quad z=x_1+\mathrm{i}x_2 \tag{84}$$

Defining the potential, electric displacement and magnet induction function

$$\mathbf{U}^h=\begin{Bmatrix}\phi^h\\ \psi^h\end{Bmatrix}=2\,\mathrm{Re}\begin{Bmatrix}f_1^h(z)\\ f_2^h(z)\end{Bmatrix},\quad \boldsymbol{\phi}^h=2\,\mathrm{Re}\left\{\begin{bmatrix}b_1^h & 0\\ 0 & b_2^h\end{bmatrix}\begin{Bmatrix}f_1^h(z)\\ f_2^h(z)\end{Bmatrix}\right\} \tag{85}$$

where $b_1^h=-\mathrm{i}\kappa^h$, $b_2^h=-\mathrm{i}\mu^h$, we have

$$\Sigma_1^h=\{D_1^h,B_1^h\}^T=-\boldsymbol{\phi}_{,2}^h,\quad \Sigma_2^h=\{D_2^h,B_2^h\}^T=\boldsymbol{\phi}_{,1}^h \tag{86}$$

Using the above expression, the magnetoelectroelastic boundary conditions along the surface of the hole can be written as [44]

$$\mathbf{g}^T\mathbf{U}=\mathbf{U}^h,\quad \boldsymbol{\phi}=\mathbf{g}\boldsymbol{\phi}^h \text{ on } \Gamma \tag{87}$$

$$\Sigma_{ij}\to 0 \text{ at infinity} \tag{88}$$

where

$$\mathbf{g}=\begin{bmatrix}0&0&0&1&0\\0&0&0&0&1\end{bmatrix}^T \tag{89}$$

As in [48], the single-valued mapping of the hole region, Ω_h, can be written

$$z=\frac{a+b}{2}\zeta+\frac{a-b}{2}\zeta^{-1} \tag{90}$$

The roots of $dz/d\zeta=0$ are $\zeta_{1,2}=\pm[(1-e)/(1+e)]^{1/2}$, where $e=b/a$. Thus, the mapping of the region Ω_h can be performed by excluding a straight line Γ_0 of length $2a(1-e^2)^{1/2}$ along the x_1-axis from the ellipse. In this case, the mapping function (90) will transform Γ and Γ_0 into the ring of outer and inner circles with radii $r_{\text{out}}=1$ and $r_{in}=[(1-e)/(1+e)]^{1/2}$, respectively.

To satisfy the conditions (87), the solutions $\mathbf{U}$ and $\boldsymbol{\phi}$ can be taken in the form given in Eqs. (73) and (74), and $\mathbf{U}^h$ and $\boldsymbol{\phi}^h$ are assumed as

$$\mathbf{U}^h = 2\,\mathrm{Re}\sum_{k=1}^{2}[\mathbf{f}_k^h(\mathbf{z})\mathbf{q}_{hk}] \tag{91}$$

$$\boldsymbol{\phi}^h = 2\,\mathrm{Re}\sum_{k=1}^{2}[\mathbf{B}^h\mathbf{f}_k^h(\mathbf{z})\mathbf{q}_{hk}] \tag{92}$$

where

$$\mathbf{B}^h = \begin{bmatrix} -i\kappa^h & 0 \\ 0 & -i\mu^h \end{bmatrix} \tag{93}$$

$$\begin{aligned} f_1^h(z) &= a[q_0F_1(\zeta)+q_0F_2(\zeta)+\bar{q}_0F_3(\zeta)+\bar{q}_0F_4(\zeta)]/2 \\ f_2^h(z) &= i\tau b[-q_0F_1(\zeta)+q_0F_2(\zeta)-\bar{q}_0F_3(\zeta)+\bar{q}_0F_4(\zeta)]/2 \end{aligned} \tag{94}$$

The condition (87) provides

$$\begin{aligned} &2\,\mathrm{Re}[\mathbf{g}^T(\mathbf{A}\mathbf{q}_1+\mathbf{c})] = 2\,\mathrm{Re}[\mathbf{q}_{h1}], \\ &2\,\mathrm{Re}[\mathbf{B}\mathbf{q}_1+\mathbf{d}] = 2\,\mathrm{Re}[\mathbf{g}\mathbf{B}^h\mathbf{q}_{h1}] \end{aligned} \tag{95}$$

$$\begin{aligned} &2\,\mathrm{Re}[\mathbf{g}^T(\mathbf{A}\mathbf{P}\mathbf{q}_2+\mathbf{c}\tau)] = 2\,\mathrm{Re}[\mathbf{q}_{h2}\tau], \\ &2\,\mathrm{Re}[\mathbf{B}P\mathbf{q}_2+\mathbf{d}\tau] = 2\,\mathrm{Re}[\mathbf{g}\mathbf{B}^h\mathbf{q}_{h2}\tau] \end{aligned} \tag{96}$$

Solving Eqs. (95) and (96) yields

$$\mathbf{q}_1 = \mathbf{W}V, \quad \mathbf{q}_{h1} = \mathbf{g}^T[\mathbf{A}\mathbf{W}\mathbf{V}+\mathbf{c}] \tag{97}$$

$$\mathbf{q}_2 = \tau\mathbf{P}^{-1}\mathbf{W}\mathbf{V}, \quad \mathbf{q}_{h2} = \mathbf{q}_{h1} \tag{98}$$

where

$$\mathbf{W} = \mathbf{B}-\mathbf{g}\mathbf{B}^h\mathbf{g}^T\mathbf{A}, \quad \mathbf{V} = \mathbf{g}\mathbf{B}^h\mathbf{g}^T\mathbf{c}-\mathbf{d} \tag{99}$$

A crack of length $2a$ can be formed by letting the minor axis b of the ellipse approach zero. The solutions for a crack in an infinite magnetoelectroelastic plate can then be obtained from the formulation above by setting $b=0$. In this case, Eqs. (63), (64), and (90) are reduced to

$$z_t = \frac{a}{2}(\zeta_t+\zeta_t^{-1}), \quad a_{1\tau} = a_{2\tau} = \frac{a}{2} \tag{100}$$

$$z_k = \frac{a}{2}(\zeta_k+a_{2k}\zeta_k^{-1}), \quad a_{1k} = a_{2k} = \frac{a}{2} \tag{101}$$

$$z = \frac{a}{2}\left(\zeta+\zeta^{-1}\right) \tag{102}$$

Substituting the expressions (100)–(102) into Eqs. (69)–(77), the corresponding solution for a permeable crack can be obtained. We omit those details here since it is tedious and algebraic. Similar results for a permeable crack has been discussed elsewhere [2].

5. Conclusion

The problem of various defects embedded in an infinite magnetoelectroelastic solid subjected to thermal loading has been addressed within the framework of in-plane magnetoelectroelastic interactions. A family of closed-form thermomagnetoelectroelastic Green's functions for problems of defects in a magnetoelectroelastic solid has been derived through the use of Stroh's formalism and conforming mapping. The defects may be of an elliptic hole or a Griffith crack, half-plane boundary, bimaterial interface, or rigid inclusion. These Green's functions satisfy the related boundary or interface conditions. In the case of hole problem, both permeable and impermeable boundaries are considered. The Griffith crack of finite length $2a$ can be generated by setting the minor semi-axis b at zero. Thus their Green's functions can be obtained from the related solutions of the elliptical hole problem. The Green's functions obtained can be used to establish boundary element formulation and to analyze fracture behavior due to the defects mentioned above.

References

[1] Mura T. Micromechanics of defects in solids. 2nd ed. Dordrecht: Martinus Nijhoff Publishers; 1987.
[2] Qin QH. Fracture mechanics of piezoelectric materials. Southampton: WIT Press; 2001.
[3] Qin QH, Mai YW. BEM for crack-hole problems in thermopiezoelectric materials. Eng Frac Mech 2002;69:577–88.
[4] Benveniste Y. The determination of the elastic and electric-fields in a piezoelectric inhomogeneity. J Appl Phys 1992;72:1086–95.
[5] Chen T. Green's functions and the non-uniform transformation problem in a piezoelectric medium. Mech Res Commun 1993;20:271–8.
[6] Chen T, Lin FZ. Numerical evaluation of derivatives of the anisotropic piezoelectric Green's function. Mech Res Commun 1993;20:501–6.
[7] Dunn ML. Electroelastic Green's functions for transversely isotropic media and their application to the solution of inclusion and inhomogeneity problems. Int J Eng Sci 1994;32:119–31.
[8] Pan E. A BEM analysis of fracture mechanics in 2D anisotropic piezoelectric solids. Eng Anal Boundary Elements 1999;23:67–76.
[9] Sosa HA, Castro MA. On concentrated load at boundary of a piezoelectric half-plane. J Mech Phys Solids 1994;42:1105–22.
[10] Norris AN. Dynamic Green's functions in anisotropic, thermoelastic, and poroelastic solids. Proc R Soc Lond 1994;A447:175–88.
[11] Khutoryansky NM, Sosa HA. Dynamic representation formulas and fundamental solutions for piezoelectricity. Int J Solids Struct 1995;32:3307–25.
[12] Fan H, Sze KY, Yang W. Two dimensional contact on a piezoelectric half space. Int J Solids Struct 1996;33:1305–15.

[13] Qin QH. Green's function and its application for piezoelectric plate with various openings. Arch Appl Mech 1999;69:133–44.
[14] Qin QH, Mai YW. Crack branch in piezoelectric bimaterial system. Int J Eng Sci 2000;38:673–93.
[15] Pan E, Yuan FG. Three-dimensional Green's functions in anisotropic piezoelectric bimaterials. Int J Eng Sci 2000;38:1939–60.
[16] Pan E, Tonon F. Three-dimensional Green's functions in anisotropic piezoelectric solids. Int J Solids Struct 2000;37:943–58.
[17] Dunn ML, Wienecke HA. Green's function for transversely isotropic piezoelectric solids. Int J Solids Struct 1996;33:4571–81.
[18] Gao CF, Fan WX. Green's functions for the plane problem in a half-infinite piezoelectric medium. Mech Res Commun 1998;25:69–74.
[19] Dunn ML, Wienecke HA. Half-space Green's function for transversely isotropic piezoelectric solids. J Appl Mech 1999;66:675–9.
[20] Gao CF, YU JH. Two-dimensional analysis of a semi-infinite crack in piezoelectric media. Mech Res Commun 1998;25:695–700.
[21] Chen BJ, Xiao ZM, Liew KM. On the interaction between a semi-infinite anti-crack and a screw dislocation in piezoelectric solid. Int J Eng Sci 2004;42:1–11.
[22] Ding HJ, Chen B, Liang J. On the green's functions for two-phase transversely isotropic piezoelectric media. Int J Solids Struct 1997;34:3041–57.
[23] Gao CF, Kessler H, Balke H. Green's function for anti-plane deformations of a circular arc-crack at the interface of piezoelectric materials. Arch Appl Mech 2003;73:467–80.
[24] Liu JX, Wang B, Du SY. Line force, charge and dislocation in anisotropic piezoelectric materials with an elliptic hole or a crack. Mech Res Commun 1997;24:399–405.
[25] Lu P, Williams FW. Green's function of piezoelectric materials, with an elliptic hole or inclusion. Int J Solids Struct 1998;35:651–64.
[26] Gao CF, Fan WX. Green's function for generalized 2D problems in piezoelectric media with an elliptic hole. Mech Res Commun 1998;25:685–93.
[27] Lu P, Tan MJ, Liew KM. A further investigation of Green's functions for a piezoelectric media with a cavity or a crack. Int J Solids Struct 2000;37:1065–78.
[28] Gao CF, Fan WX. A general solution for the plane problem in piezoelectric media with collinear cracks. Int J Eng Sci 1999;37:347–63.
[29] Gao CF, Wang MZ. Green's function of an interface crack between two dissimilar piezoelectric media. Int J Solids Struct 2001;38:5323–34.
[30] Gao CF, Wang MZ. General treatment on mode III interfacial crack problems in piezoelectric materials. Arch Appl Mech 2001;71:296–306.
[31] Qin QH. Thermoelectroelastic Green's function for a piezoelectric plate containing an elliptic hole. Mech Mater 1998;30:21–9.
[32] Qin QH, Mai YW. Thermoelectroelastic Green's function and its application for bimaterial of piezoelectric materials. Arch Appl Mech 1998;68:433–44.
[33] Qin QH. Green's function for thermopiezoelectric materials with holes of various shapes. Arch Appl Mech 1999;69:406–18.
[34] Qin QH. Thermoelectroelastic Green's function for thermal load inside or on the boundary of an elliptic inclusion. Mech Mater 1999;31:611–26.
[35] Qin QH. Thermoelectroelastic solution on elliptic inclusions and its application to crack-inclusion problems. Appl Mathe Model 2000;25:1–23.
[36] Pan E. Three dimensional Green's functions in anisotropic magnetoelectroelastic bimaterials. Z Angew Math Phys 2002;53:815–38.
[37] Pan E. Exact solution for simply supported and multilayered magneto-electro-elastic plates. J Appl Mech 2001;68:607–18.
[38] Pan E, Heyliger PR. Exact solutions for magneto-electro-elastic laminates in cylindrical bending. Int J Solids Struct 2003;40:6859–76.
[39] Soh AK, Liu JX, Hoon KH. Three-dimensional Green's functions for transversely isotropic magnetoelectroelastic solids. Int J Nonlinear Sci Num Simul 2003;4:139–48.
[40] Huang JH, Chiu YH, Liu HK. Magneto-electro-elastic Eshelby tensors for a piezoelectric–piezomagnetic composite reinforced by ellipsoidal inclusions. J Appl Phys 1998;83:5364–70.
[41] Li JY, Dunn ML. Anisotropic coupled-field inclusion and inhomogeneity problems. Philos Mag A 1998;77:1341–50.
[42] Li JY. Magneto-electro-elastic multi-inclusion and inhomogeneity problems and their applications in composite materials. Int J Eng Sci 2000;38:1993–2011.
[43] Hou P, Andrew YTL, Ding HJ. The elliptical Hertzian contact of transversely isotropic magneto-electro-elastic bodies. Int J Solids Struct 2003;40:2833–50.
[44] Liu J, Liu X, Zhao Y. Green's functions for anisotropic magnetoelectroelastic solids with an elliptical cavity or a crack. Int J Eng Sci 2001;39:1405–18.
[45] Barnett DM, Lothe J. Dislocations and line charges in anisotropic piezoelectric insulators. Phys Stat Sol(b) 1975;67:105–11.
[46] Aboudi J. Micromechanical analysis of fully coupled electro-magneto-thermo-elastic multiphase composites. Smart Mater Struct 2001;10:867–77.
[47] Gao CF, Kessler H, Balke H. Fracture analysis of electromagnetic thermoelastic solids. Euro J Mech A/Solids 2003;22:433–42.
[48] Qin QH. A new solution for thermopiezoelectric solid with an insulated elliptic hole. Acta Mech Sinica 1998;14:157–70.